Journal of Nuclear Materials 406 (2010) 119–126

Contents lists available at ScienceDirect

Journal of Nuclear Materials

journal homepage: www.elsevier.com/locate/jnucmat

Calibration of three-parameter Weibull stress model for 15Kh2NMFA RPV steel

Robert Beleznai [a,*], Gyöngyvér B. Lenkey [a], Dana Lauerova [b]

[a] Bay Zoltán Foundation for Applied Research, Institute for Logistics and Production Systems, Hungary
[b] Nuclear Research Institute, Rez plc, Czech Republic

A B S T R A C T

Weibull stress model represents a basic local approach model used in the ductile-to-brittle transition region for description and prediction of cleavage fracture for materials of both PWR and WWER reactor pressure vessels. In the Weibull stress model used most frequently until now [1], the parameters are determined by a calibration procedure using the fracture toughness values of high and low constraint specimens. In the present paper, the results of SEN(B) pre-cracked specimens of $10 \times 20 \times 120$ mm size, with deep and shallow cracks, are utilized. Specimens were made of material of WWER-1000 reactor pressure vessel, and were tested at Nuclear Research Institute Rez. Determination of Weibull stress was performed for both the case of including plastic strain correction into the Weibull stress formula and without it.

1. Introduction

In the three-parameter Weibull stress model of cleavage fracture, the relationship between the fracture probability and Weibull stress σ_w is described by the following equation:

$$P_f(\sigma_w) = 1 - \exp\left[-\frac{1}{V_0}\int_{\bar{V}}\left(\frac{\sigma_1}{\sigma_u}\right)^m dV\right] = 1 - \exp\left[-\left(\frac{\sigma_w - \sigma_{w\text{-min}}}{\sigma_u - \sigma_{w\text{-min}}}\right)^m\right] \quad (1)$$

The definition of Weibull stress without strain correction is as follows:

$$\sigma_w = \left[\frac{1}{V_0}\int_{\bar{V}}\sigma_1^m dV\right]^{1/m} \quad (2)$$

where m is the shape parameter of Weibull distribution (Weibull-modulus), σ_u is the scaling parameter, $\sigma_{w\text{-min}}$ is the minimum σ_w-value at which macroscopic cleavage fracture becomes possible, σ_1 is the maximum principal stress, V_0 is the reference volume, and integration is performed over volume $\bar{V}$ representing the plastic zone relevant to the crack.

The purpose of this work was to determine the parameters of the Weibull stress model (m, σ_u, $\sigma_{w\text{-min}}$) in case of unirradiated WWER-1000 type reactor pressure vessel steel, using the calibration procedure described in [1]. SEN(B) specimens containing deep and shallow crack were tested at NRI Rez, and finite element analyses were conducted in Bay Zoltan Foundation (BZF) and Nuclear Research Institute Rez (NRI) to calculate the stress distribution, Weibull stress and J-integral values. Results of 3D finite element models obtained by both institutes were compared.

Total number of 39 SEN(B) specimens made of WWER-1000 reactor pressure vessel material were tested in NRI Rez, but for the purpose of evaluation using Weibull stress model only 12 of them (tested at temperature $T = -130$ °C) were selected.

2. Specimen geometry and material properties used in FE calculations

Testing specimens were of SEN(B) type, without side-grooving, with dimensions $10 \times 20 \times 120$ mm ($B \times W \times L$). They contained either shallow or deep crack (six specimens with deep crack, six specimens with shallow crack), the individual crack depths as well as fracture toughness data are given in Tables 1 and 2.

Specimens were made of base material of WWER-1000 reactor pressure vessel, i.e. 15Kh2NMFA steel (in as-received condition). Mechanical properties of this steel were provided by NRI for temperatures 24, −30, −90, −150 and −190 °C; for test temperature $T = -130$ °C they were determined by interpolation.

In FE calculations, Young-modulus and Poisson's ratio were taken are as follows:

- $E = 210$ GPa.
- $\nu = 0.3$.

True stress–true plastic strain curve appropriate for temperature $T = -130$ °C may be seen in Fig. 1.

* Corresponding author. Tel.: +36 46 560 120; fax: +36 46 422 786.
E-mail address: beleznai.robert@bay-logi.hu (R. Beleznai).

0022-3115/$ - see front matter © 2010 Elsevier B.V. All rights reserved.
doi:10.1016/j.jnucmat.2010.04.027

Table 1
Fracture toughness data for shallow crack specimens.

Specimen ID	a (mm)	$T = -130$ °C	
		J_c (kJ/m^2)	K_{Jc} (M Pa m$^{1/2}$)
69945	1.8	206.29	218.19
69946	2.0	31.19	84.84
69947	1.6	185.40	206.84
69948	1.4	155.86	189.65
69949	1.6	118.60	165.44
69950	1.4	180.57	204.13

Table 2
Fracture toughness data for deep crack specimens.

Specimen ID	a (mm)	$T = -130$ °C	
		J_c (kJ/m^2)	K_{Jc} (M Pa m$^{1/2}$)
69857	9.8	48.50	105.79
69858	9.8	56.89	114.58
69859	9.8	26.17	77.71
69860	9.9	11.53	51.58
69861	9.8	38.41	94.15
69862	9.8	17.40	63.37

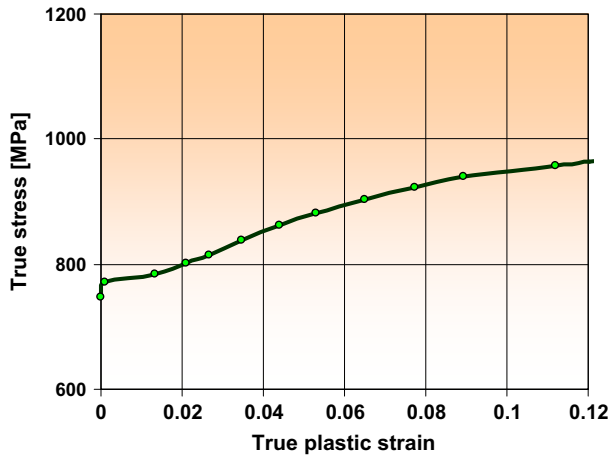

Fig. 1. True stress–true plastic strain curve at $T = -130$ °C for 15Kh2NMFA RPV material.

The following proportionality limit at temperature $T = -130$ °C was used in the FE calculations:

- $R_{p0,0} = 748$ MPa.

3. Experimental results and determination of MC reference temperature T_0

All specimens fractured by cleavage, no ductile tearing prior cleavage was observed. The appropriate fracture toughness data, for both shallow and deep crack specimens, may be seen in Fig. 2. Test temperature of evaluated specimens $T = -130$ °C lies approx. 20 °C below Master Curve T_0 [2] determined for this material, $T_0 = -111$ °C. Determination of T_0 was made based on results of fracture toughness tests of in total 19 SEN(B) specimens of dimensions $10 \times 20 \times 120$ mm, containing deep crack, and tested at three different temperatures −100 °C, −120 °C and −130 °C, see Fig. 3.

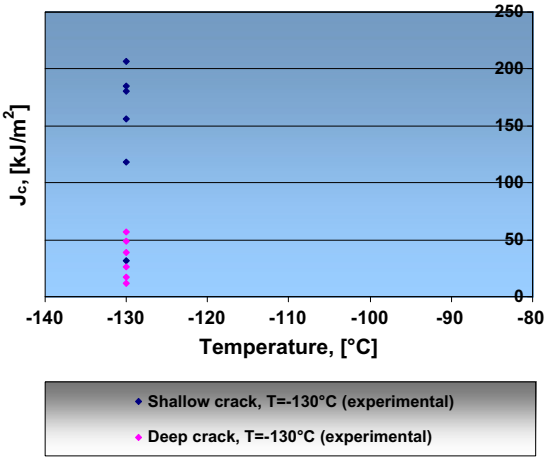

Fig. 2. Fracture toughness data for shallow and deep crack specimens of 15Kh2NMFA RPV material.

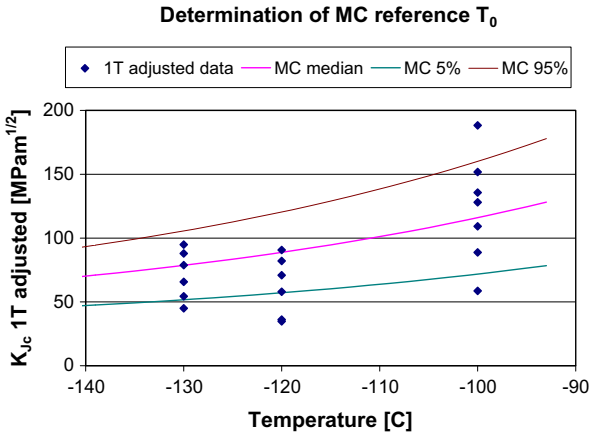

Fig. 3. Determination of MC T_0 based on deep crack specimens tests.

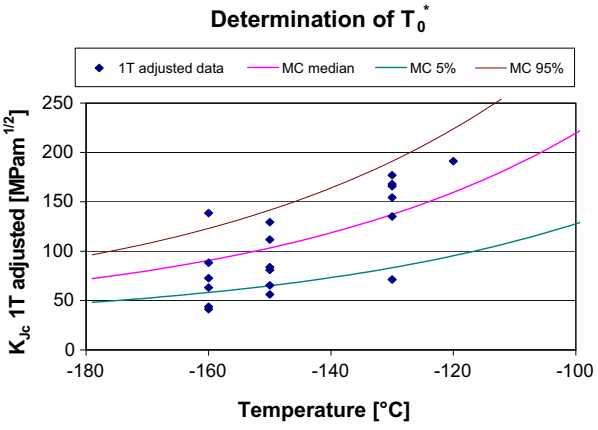

Fig. 4. Determination of MC T_0^* based on shallow crack specimens tests.

3.1. Note 1

In Fig. 3, toughness data points at temperature −130 °C are a little higher than at −120 °C. Similar phenomenon was sometimes observed for materials of RPV of WWER type reactors in lower part of ductile-to-brittle transition region, and it is usually explained as natural scatter of fracture toughness in transition region. However, some experts in NRI [4] consider this phenomenon as consequence of twinning. Twinning occurs at sufficiently low temperatures and

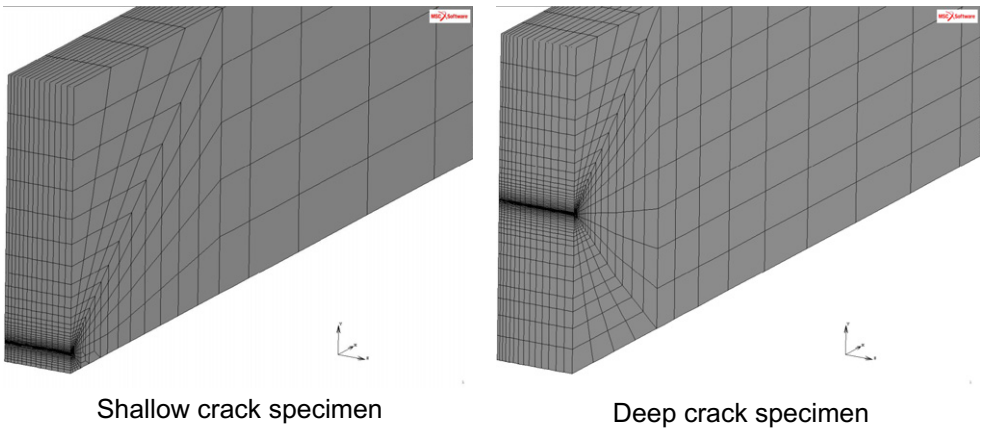

Fig. 5. Finite element model for shallow and deep crack specimen, BZF.

since it consumes energy supplied to the specimen during loading, fracture toughness becomes higher. It is a hypothesis, but no other explanation is available (besides of scatter).

The shift of T_0 due to "shallow crack effect" for this material was evaluated as well, $\Delta T_0 = 41$ °C, corresponding to average a/W ratio = 0.08 (T_0^* for shallow cracks was determined as $T_0^* = -152$ °C, see Fig. 4).

4. Finite element models

In both BZF and NRI, 3D finite element models of specimens were developed for the calculations. In BZF, MSC.MARC 2007R1 code was used for FE calculation, in NRI, FE analysis was performed using FE code SYSTUS. In both cases, 20-node-elements were used for construction of FE meshes, and symmetry conditions were applied – only one quarter of the specimen was modeled (Fig. 5).

In the calibration procedure, the small scale yielding (SSY) model was used [1], with a convenient reference thickness. In both BZF and NRI, the SSY model was constructed as a 2D plane strain model with crack modeled as a notch with radius of 1 μm (NRI) or 25 μm (BZF), see Fig. 6.

In BZF, four different FE models of specimens were constructed according to real crack depths: 1.4 mm, 1.6 mm, 1.8 mm (for shallow crack models) and 9.8 mm (for deep crack model). All specimens models had blunted crack tip with a radius $\rho = 25$ μm. Around the crack tip the mesh was refined significantly (Fig. 7), element edge length around the crack tip was 0.0046 mm; the equivalent von Mises stress distribution for deep crack specimen 69858 may be seen in Fig. 8 for the load level of fracture.

In NRI, six different FE models were developed differing by crack depths: four models for shallow crack specimens (crack depth 1.39 mm, 1.56 mm, 1.76 mm, and 1.97 mm) and two models for deep crack specimens (crack depth 9.83 mm and 9.94 mm). In each case, the crack was modeled as a sharp one, with element size near the crack front of about 0.01 mm.

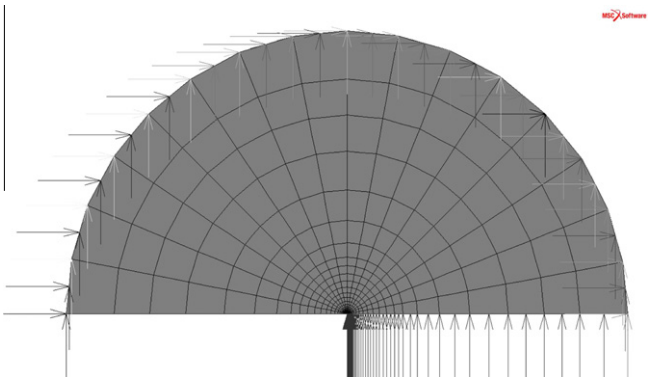

Fig. 6. SSY boundary layer model, BZF.

4.1. Note 2

Effect of FE mesh refinement on parameters m and σ_u was tested in NRI for case of 2-parametric Weibull model and it was found that its effect is very small (practically negligible). Of course, this statement is valid only under assumption that 3D FE meshes with sufficiently small element size near crack front are used (with element size near crack front about 0.01 mm or smaller).

In BZF, the problem of mesh dependence of the results was examined for the case of 3D FE model of a shallow crack specimen with crack depth 1.4 mm. The mesh was refined around the crack tip in an extended zone, as can be seen from Fig. 9. Element edge length around the crack tip was 0.0023 mm. Using Weibull stress values of the new model, a comparison with previous Weibull stress values was done, and the difference was found to be negligible, in particular, approx. 1.4% (Table 3). Due to such small difference, the results were considered as mesh independent. The final calculation was then performed using the "normal" mesh, i.e. mesh with element size near the crack front of 0.0046 mm.

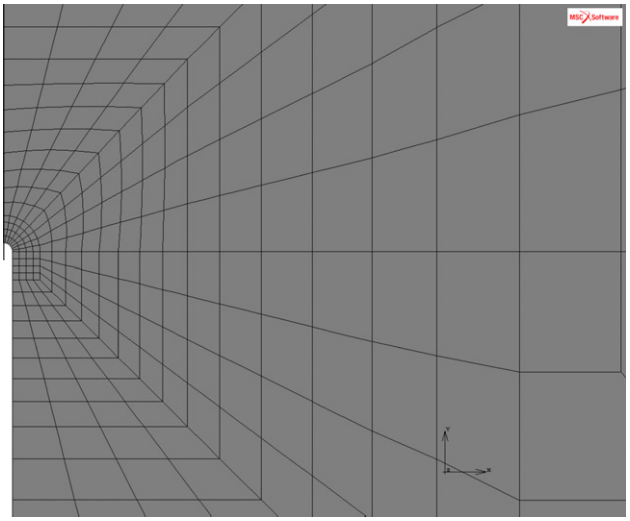

Fig. 7. Fine mesh around the crack tip of the specimen in case of "normal" mesh, BZF.

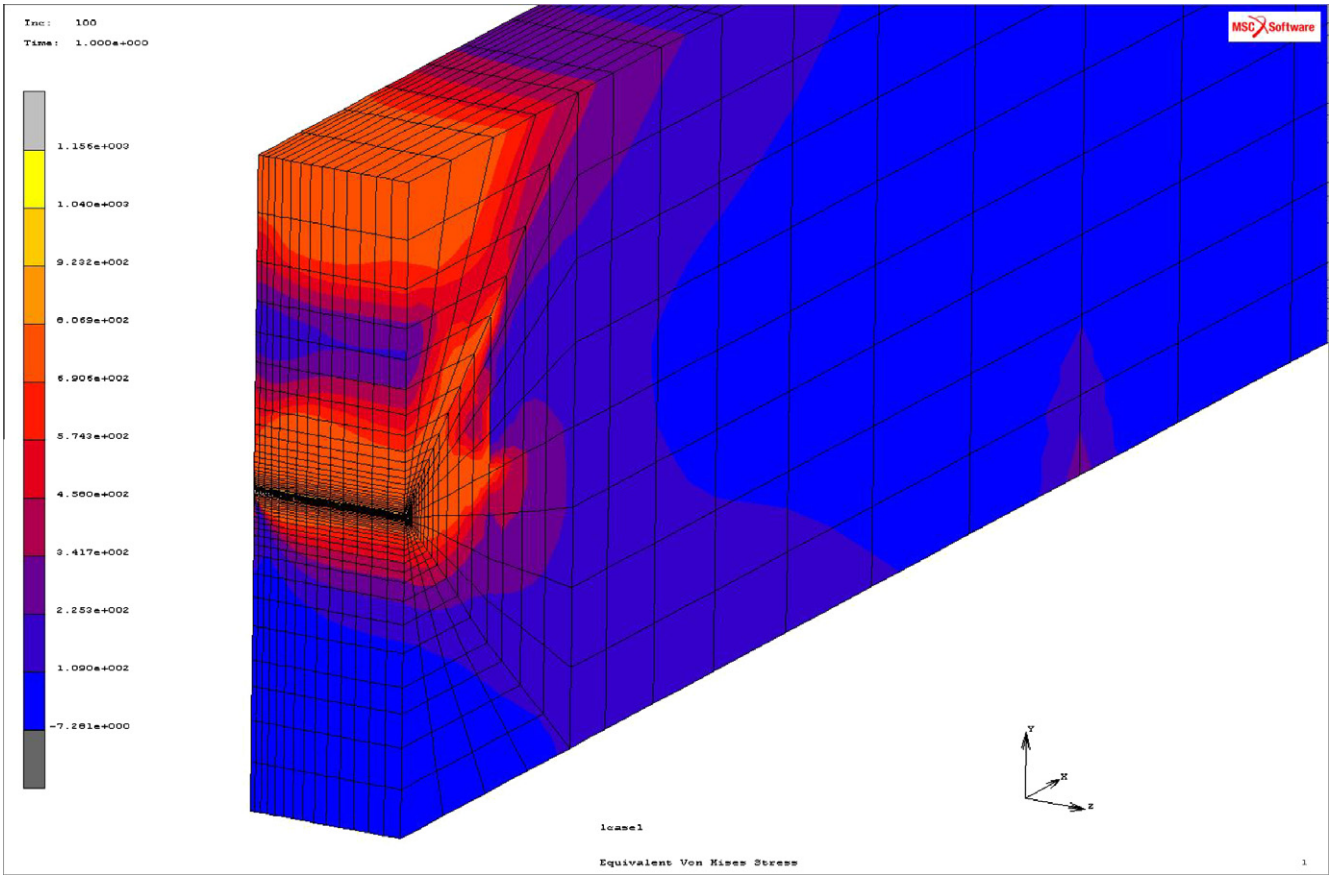

Fig. 8. Equivalent von Mises stress distribution for deep crack specimen, BZF.

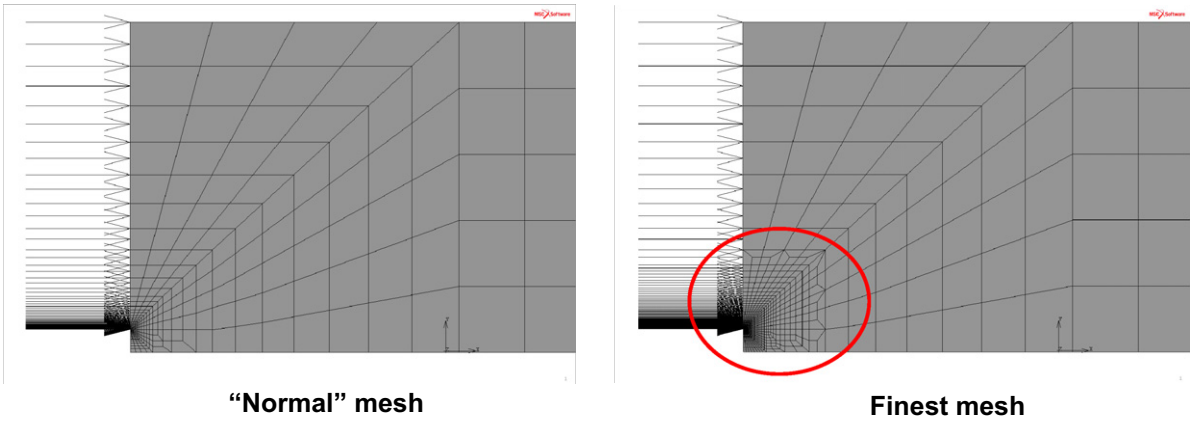

Fig. 9. Refined mesh for verification of the mesh independent results (for sufficiently refined meshes).

Table 3
Test on Weibull stress mesh independency (for sufficiently refined meshes).

Specimen ID	Weibull stress (MPa)		Error (%)
	Finest mesh	"Normal" mesh	
69948	5156.656	5227.936	1.36
69950	5210.252	5284.127	1.40

For calculation of *J*-integral, the *G*-theta method (3D) implemented in SYSTUS was used in NRI.

In case of BZF, the *J*-values in the SSY model were determined using Rice contour integral, with procedure for its calculation implemented in Marc. For 3D specimen models, the *J*-values were not determined, since there was no necessity of determining them: in the calibration procedure the experimental values J_c (provided by NRI) were used.

In NRI, moment of fracture in FE calculation was determined based on force vs. CMOD curve, using experimental value of CMOD. In majority of cases, very good accordance between experimental and calculated records was reached (Fig. 10).

In BZI, moment of fracture was determined based on force vs. CMOD curve using value of force, since FE model of BZF did not enable to compare the calculated value of CMOD directly to the experimental one (experimental CMOD was measured in a small

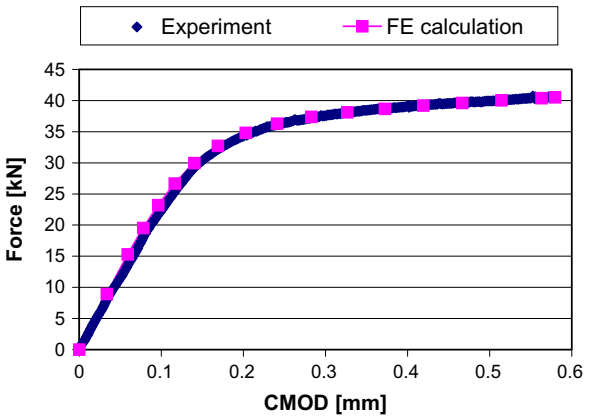

Fig. 10. Comparison of experimental and calculated force vs. CMOD curve for shallow crack specimen 69950 NRI.

distance from the specimen upper surface, this detail was not modeled in BZF FE models).

In both BZF and NRI, flow theory with large deformations (updated Lagrangian formulation) and von Mises condition of plasticity was used for modeling plastic properties of the material.

5. Basic idea of Weibull model approach and the relevant calibration procedure

Since 1983 when Beremin group presented the famous paper [3], Weibull stress formula (2) has been widely used as measure of the probability of cleavage failure. The importance of the Weibull model approach for description/prediction of cleavage fracture was still enhanced when effect of constraint on fracture toughness was recognized and began to be studied.

In general, the main idea of three-parameter Weibull model approach may be briefly described as follows: Such values of parameters m, σ_u and $\sigma_{w\text{-min}}$ exist that after transforming J_c-values (for two sets of specimens – with deep and shallow cracks) into σ_w-values using σ_w vs. J relations determined by FE calculations separately for deep and shallow crack sets, the obtained two groups of σ_w-values belong (in the SSY model configuration) to the same three-parametric Weibull distribution with these (potentially existing) values of parameters. The calibration procedure following further in the text describes an iteration procedure serving for finding these values of parameters. However, in our particular case, the 3rd parameter, $\sigma_{w\text{-min}}$, was not calibrated based on experiments, but it was taken as corresponding to fixed value of $K_{\min} = 20$ MPam$^{1/2}$ (in the SSY model configuration). This was done with reference to Master Curve concept [2] within which value $K_{\min} = 20$ M Pa m$^{1/2}$ is assigned zero probability of fracture. Thus, this 3rd parameter $\sigma_{w\text{-min}}$ is not a real independent parameter of the three-parametric Weibull distribution used in this paper.

The calibration procedure is based on the work [1], and includes the following steps:

1. Generating FE models for shallow and deep crack specimens, and SSY boundary layer model.
2. Determine the principal stress over the process zone at the fracture. The definition of the process zone was the following: the volume inside the contour where the total equivalent (or cumulative[1]) plastic strain is above 0.002. Only plastic zone pertinent to the crack front was taken into account.
3. Assume an m value. Compute the σ_w vs. J history for deep and shallow crack specimens, and SSY model configurations. For the σ_w calculation $V_0 = 0.001$ mm^3 reference volume was used.
4. Determine $\sigma_{w\text{-min}}$ value (at $K_{\min} = 20$ MPam$^{1/2}$ in the SSY model), and obtain the σ_w^* vs. J curves for each crack configuration, where $\sigma_w^* = \sigma_w - \sigma_{w\text{-min}}$.
5. Correct toughness distributions for deep crack and shallow crack specimens to SSY configuration using the toughness scaling model based on equal σ_w^* values. Illustration of this procedure can be seen in Fig. 11, taken from [1].
6. Estimate β_{SSY} for the two distributions defined by the constraint-corrected toughness values from deep and shallow crack specimens:

$$\beta_{SSY} = \left(\frac{1}{n}\sum_{i=1}^{n} J_{(i)-SSY}^2\right)^{1/2} \tag{3}$$

where n is the number of the fracture toughness values in the data set.

7. Define an error function as

$$R(m) = (\beta_{SSY}^{shallow} - \beta_{SSY}^{deep})/\beta_{SSY}^{deep} \tag{4}$$

8. If $R(m) \neq 0$, repeat the points from 3 to 8 for additional m-values. The Weibull-modulus is obtained within a small tolerance of $R(m) = 0$.
9. Compute the σ_u value. After m is determined, σ_u equals the Weibull stress value at $J_c = \beta_{SSY}^{deep} = \beta_{SSY}^{shallow}$ in the SSY configuration with a specified reference thickness.

6. Calibration of the Weibull model parameters for unirradiated WWER-1000 type RPV material

The calibration procedure was applied to WWER-1000 type RPV material for temperature $T = -130$ °C, as described in points 1–9 above. The reference thickness of SSY solution was taken 5 mm, i.e. equal to the thickness of one-quarter-model of the specimens. Also all values of Weibull stress presented in the figures further in the text are relevant to thickness of 5 mm.

The results of the 3D FE calculations were used in the calibration software to determine the Weibull stress model parameters. In BZF, the calibration software was written in Fortran language. In NRI, the appropriate values were extracted from SYSTUS and processed in Excel to determine σ_w; also the whole calibration procedure (finding of m, $\sigma_{w\text{-min}}$, and σ_u) was performed in Excel.

The calibration procedure was performed in two versions:

(a) with using Weibull stress formula (2), i.e. with no strain correction
(b) using the following Beremin strain correction of Weibull stress formula [3]

$$\sigma_w = \left[\frac{1}{V_0}\int_V \sigma_1^m \exp\left(\frac{-m\cdot\varepsilon_1}{2}\right)dV\right]^{1/m} \tag{5}$$

where ε_1 is (total) strain tensor component in direction of maximum principal stress.

In both cases (a) and (b), the integral in Eq. (2) or (5) was calculated numerically as a sum (over all mesh elements of plastic zone pertinent to the crack front) of average values of appropriate quantities in the element multiplied by volume of the element. I.e., no special criterion for selection of the elements over which the integration is performed (other than criterion of plasticity: total

[1] Total plastic strain was used in BZF, cumulative plastic strain in NRI. In NRI and BZF, a comparison of both approaches was performed showing that the difference in results is negligible.

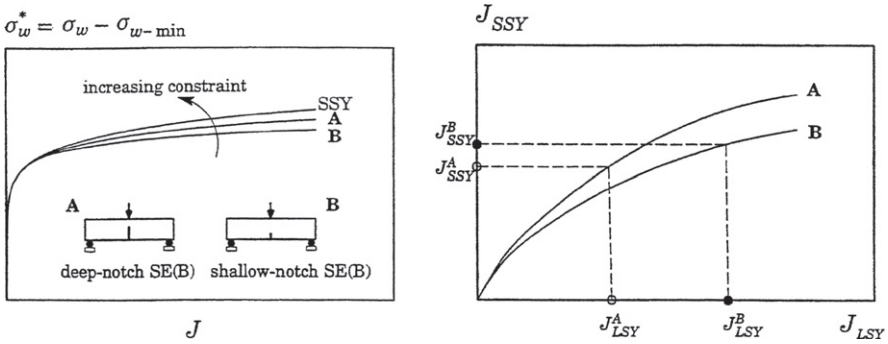

(a) σ^*_W vs. J curves showing the evolution of σ^*_W as J increases

(b) Toughness scaling diagram (J^{SSY} vs. J^A and J^B), each pair of J-values on the curve corresponds to the same σ^*_W - value

Fig. 11. Illustration of toughness scaling between deep and shallow crack configurations and SSY model configuration [1].

Table 4
Calibrated Weibull parameters for WWER-1000 type RPV steel.

	m	$\sigma_{w\text{-min}}$[a] (MPa)	σ_u[a] (MPa)
3D calculation without strain correction, BZF	8.4	2046	4464
3D calculation without strain correction, NRI	8.25	2217	4568
3D calculation with Beremin (total) strain correction (5), BZF	8.1	2052	4553
3D calculation with Beremin (total) strain correction (5), NRI	7.9	2224	4731

[a] Values of $\sigma_{w\text{-min}}$ and σ_u are relevant to 5 mm of crack front length.

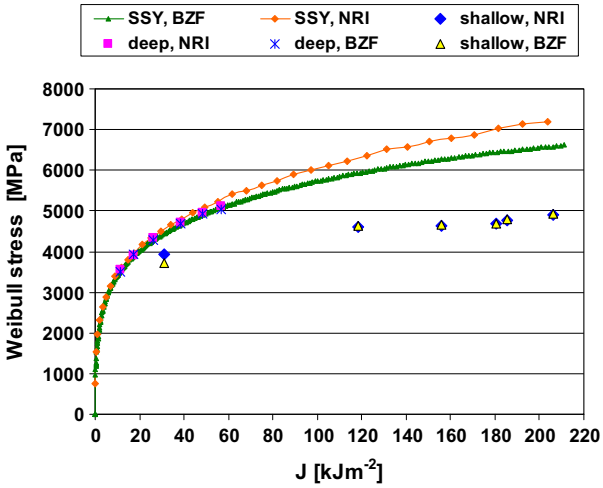

Fig. 12. Comparison of Weibull stress values obtained by BZF and NRI for the same m (m = 8.25), for SSY model and for shallow and deep crack specimens at fracture.

equivalent/cumulative plastic strain $\geqslant$0.002) was used; only plastic zone relevant to the crack was considered.

The results obtained by BZF and NRI from the respective calibration procedures are summarized in Table 4. From this table it is seen that the results obtained by BZF do not differ significantly from those ones reached in NRI. In Figs. 12–18, main results as well as some details of the performed calibration procedures are shown.

In Fig. 12, comparison of Weibull stress values obtained by the two institutes for the same m (m = 8.25) is seen. In this figure, both development of Weibull stress with increasing J for the SSY case and Weibull stress values at fracture for deep and shallow crack specimens are plotted. A good accordance between BZF and NRI results for both SSY model and specimens may be seen from this figure. The only minor discrepancy between BZF and NRI Weibull stress is found for the shallow crack specimen 69946 that fractured at lowest load. This is, most likely, due to different crack depths modeled for this specimen in BZF (a = 1.8 mm) and NRI (a = 1.97 mm). (For shallow crack specimens, all results such as stresses, displacements etc., were found relatively highly dependent on crack depth.)

6.1. Note 3

Since in both NRI and BZF the FE models of shallow crack specimens contained slightly differing crack depths (as appropriate according to the real crack depths), the fracture values of Weibull stress for shallow crack specimens in Figs. 12 and 13 visibly do not lie on a smooth curve, as it would be the case if only one (average) crack depth was modelled for all shallow crack specimens.

Various σ_w vs. J plots are seen in Fig. 13, representing solutions for m as obtained in BZF and NRI, for the respective cases without and with Beremin strain correction of Weibull stress (Eqs. (2) and (5), respectively). The Weibull stress values provided by BZF and NRI in Fig. 13 are not directly comparable, since they are relevant to different values of m. Good accordance reached in the results of calibration procedures performed by both institutes is demonstrated in values of m, σ_u and $\sigma_{w\text{-min}}$ summarized in Table 4. In case of using Weibull stress formula with no strain correction the values of Weibull model parameters were as follows: m = 8.4, σ_u = 4464 MPa, $\sigma_{w\text{-min}}$ = 2046 MPa (BZF), and m = 8.25, σ_u = 4568 MPa, $\sigma_{w\text{-min}}$ = 2217 MPa (NRI). In case of using strain corrected Weibull stress formula the following values of Weibull model parameters were obtained: m = 8.1, σ_u = 4553, $\sigma_{w\text{-min}}$ = 2052 MPa (BZF), and m = 7.9, σ_u = 4731 MPa, $\sigma_{w\text{-min}}$ = 2224 MPa (NRI).

The failure probability vs. J_{SSY}-integral curves are presented in Figs. 14–17. These figures do not differ substantially from each other, confirming thus two facts: (1) results obtained by BZF and NRI do not differ significantly, and (2) the effect of Beremin strain correction is not large. Further, clearly visible is a little special (non-uniform) distribution of shallow crack data points along the predicted fracture probability curve in these figures, which reflects the special distribution of shallow crack data points in Fig. 4 (at

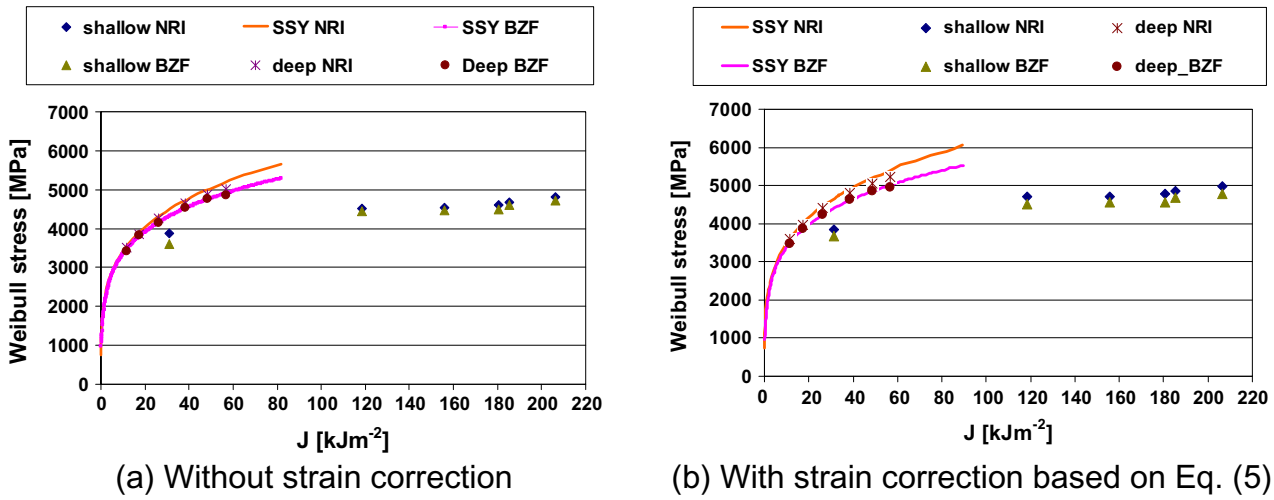

Fig. 13. Comparison of Weibull stress vs. *J*-integral plots using the different calibrated Weibull model parameters as obtained by BZF and NRI: (a) $m = 8.25$ (NRI), $m = 8.4$ (BZF) and (b) $m = 7.9$ (NRI), $m = 8.1$ (BZF).

$T = -130\,^{\circ}C$) with one data-point significantly below the five remaining ones. The accordance between the experimental data and predicted fracture probability curve may be considered as acceptable, with respect to small number of specimens taken into the evaluation.

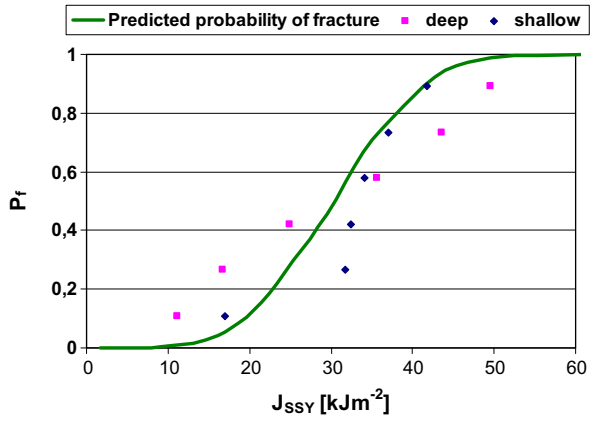

Fig. 14. Probability of fracture vs. J_{SSY}-integral plot, 3D calculation, without strain correction, NRI.

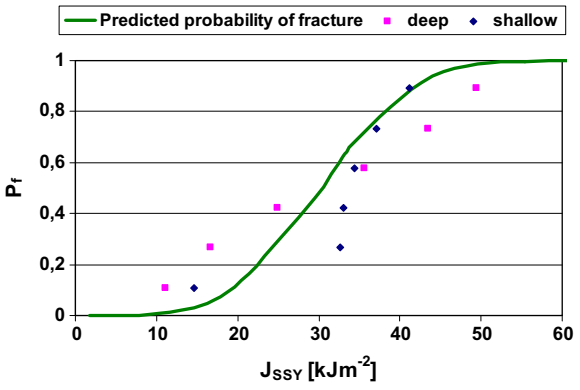

Fig. 15. Probability of fracture vs. J_{SSY}-integral plot, 3D calculation, with strain correction (5), NRI.

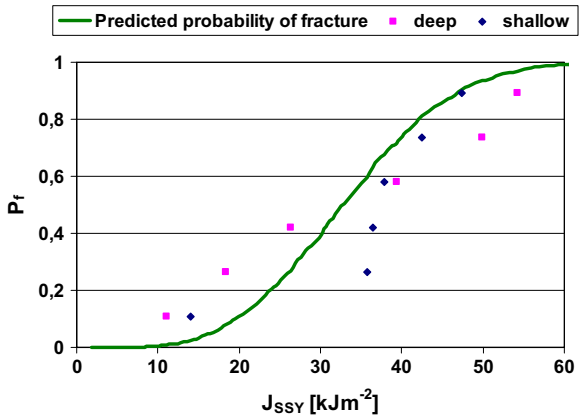

Fig. 16. Probability of fracture vs. J_{SSY}-integral plot, 3D calculation, without strain correction, BZF.

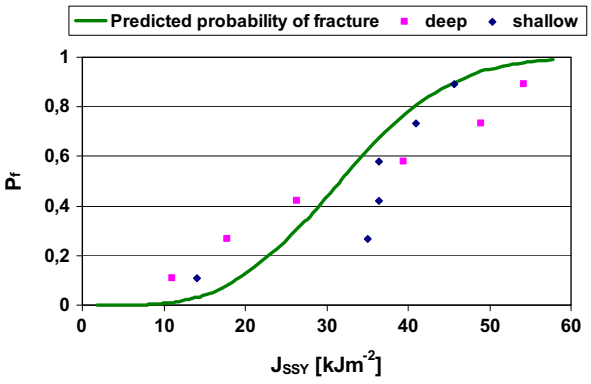

Fig. 17. Probability of fracture vs. J_{SSY}-integral plot, 3D calculation, with strain correction (5), BZF.

In Fig. 18, the error function vs. m value may be seen in cases of calibration without (Fig. 18a) and with Beremin strain correction (Fig. 18b). From this figure, it may be seen that only one solution exists in each of both cases.

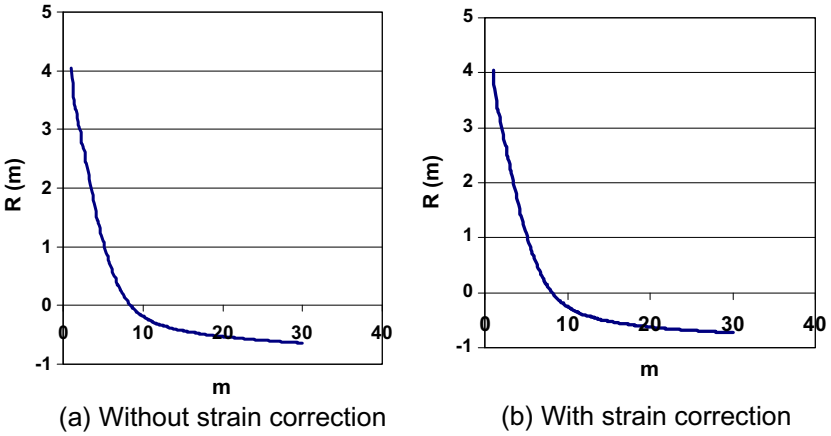

Fig. 18. Error function of the solution, BZF.

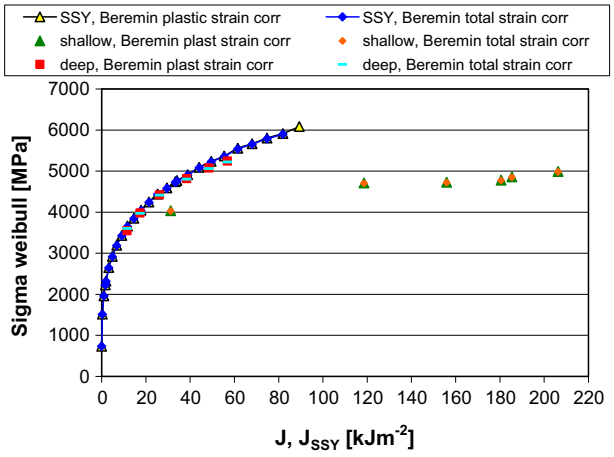

Fig. 19. Comparison of strain corrected Weibull stress values using plastic strain component as ε_1 in Eq. (5), or total strain component as ε_1 in Eq. (5), NRI.

7. Discussion – problem of the plastic strain correction

In the original Beremin paper, the strain correction formula (5) was presented, with ε_1 denoting the total strain component in direction of maximum principal stress. In Fig. 13b, Figs. 15, 17 and 18b, the results provided by both BZF and NRI were obtained based on Eq. (5) with ε_1 denoting the total strain tensor component in direction of maximum principal stress. Since in literature also the formula (5) with ε_1 denoting the plastic strain tensor component in direction of maximum principal stress was found, NRI performed a comparison to evaluate possible difference between these two interpretations. It was found that the results differ negligibly: almost the same values of Weibull stress were obtained (see Fig. 19), and in terms of Weibull model parameters m and σ_u the difference was also very small (or even zero): the same value of m ($m = 7.9$) was found for both interpretations, and $\sigma_u = 4731$ MPa was found in case of using total strain tensor component (see also Table 4) and $\sigma_u = 4743$ MPa in case of using plastic strain tensor component.

8. Conclusion

In the presented paper, the details of the Weibull stress model calibration procedures applied in BZF and NRI are shown, and, in general, a good accordance between the results of both institutes was found. In case of using Weibull stress formula without strain correction, values of m were found near eight by both institutes: $m = 8.4$ (BZF) and $m = 8.25$ (NRI). Using original Beremin strain corrected Weibull stress formula, the following values of m were found: $m = 8.1$ (BZF) and $m = 7.9$ (NRI).

When performing the calibration procedures, the authors focused mainly on numerical aspects of both determination of Weibull stress and the calibration procedure itself, as well as on mutual comparison of the results. Thus, the question of evaluating predicative capabilities of Weibull stress model was left aside. This is quite natural with respect to the fact that calibration of Weibull stress model described in the paper was made based on 12 specimens only.

Simultaneously, since the calculations in BZF and NRI were performed independently of each other, the obtained acceptable accordance in main results may be considered as a criterion of correct performing the calibration procedure, which is a necessary condition for the successful application of the calibrated model in the future.

Acknowledgements

The authors are grateful to the PERFECT (Prediction of Irradiation Damage Effects in Reactor Components) project for the financial support.

References

[1] X. Gao, R.H. Dodds Jr., R.L. Tregoning, J.A. Joyce, Fatigue Fract. Engng. Mater. Struct. 22 (1999) 481–493.
[2] ASTM E 1921-97: Standard Test Method for the Determination of Reference Temperature.
[3] F.M. Beremin, A local criterion for cleavage fracture of a nuclear pressure vessel steel, in: Metallurgical Transactions A, vol. 14A, 1983, pp. 2277–2287.
[4] D. Lauerová, Personal communication with J. Novak (NRI), 2010.